Journal of Asian Earth Sciences 34 (2009) 532–543

Contents lists available at ScienceDirect

Journal of Asian Earth Sciences

journal homepage: www.elsevier.com/locate/jaes

Late Quaternary river terrace sequences in the eastern Kunlun Range, northern Tibet: A combined record of climatic change and surface uplift

An Wang [a,b,*], Jacqueline A. Smith [c], Guocan Wang [a,b], Kexin Zhang [a,b], Shuyuan Xiang [a], Demin Liu [a]

[a] *Faculty of Earth Sciences, China University of Geosciences, Wuhan 430074, China*
[b] *State Key Laboratory of Geological Processes and Mineral Resources, China University of Geosciences, Wuhan 430074, China*
[c] *Department of Physical and Biological Sciences, The College of Saint Rose, Albany, NY 12203, USA*

ARTICLE INFO

Article history:
Received 5 February 2008
Received in revised form 2 September 2008
Accepted 8 September 2008

Keywords:
River terrace
Climate
Uplift
Quaternary
Kunlun Range
Tibet

ABSTRACT

The Kunlun Range, a reactivated orogenic belt, constitutes the northern margin of the Tibetan Plateau. The extreme relief and major landforms of the Kunlun Range are a product of late Cenozoic tectonics and erosion. However, well-developed late Quaternary terraces that occur along the northern slope of the Kunlun Range probably resulted from climatic change rather than surface uplift. The terrace sequences formed in thick Quaternary valley fills and have total incision depths of 50–60 m. Optically stimulated luminescence dating was employed to place time controls on the valley fills and associated terraces. Dating results suggest that periods of significant aggradation were synchronous between different rivers and correspond to the last glacial stage. The abrupt change from aggradation to incision occurred between 21.9 ± 2.7 and 16 ± 2.2 ka, coincident with the last glacial–interglacial transition. Additional terraces developed during the late glacial period and early to middle Holocene. Based on a broader set of chronological data in northern Tibet, at least four regional incision periods can be recognized. Chronological data, terrace elevation profiles, and climate proxy records suggest that these terracing periods were triggered by cool and/or wet climatic conditions. A geometric survey of the riverbed longitudinal profile suggests that surface uplift serves as a potential dynamic forcing for long-term incision. A model is proposed for terrace formation as a response to climatic perturbation in an uplifted mountain range.

1. Introduction

River landforms have long been of interest to researchers from a broad range of disciplines because their formation and evolution are closely related to factors that include surface uplift, climatic change, and environmental change (Fisk, 1951; Vandenberghe, 1995; Bridgland, 2000; Hsieh and Knuepfer, 2001; Starkel, 2003; Gao et al., 2005). Surface uplift is a common cause of terrace formation in tectonically active regions (Brunnacker et al., 1982; Li et al., 1996; Maddy et al., 2001). However, climatic change may be the most direct cause of terrace formation (Fisk, 1951; Chatters and Hoover, 1992) because hydrological dynamic parameters that dominate riverbed sediment aggradation and transportation (e.g., flux and flow velocity) are directly related to climatic conditions (Bull, 1991). Recent studies (Bridgland, 2000; Hsieh and Knuepfer, 2001; Maddy et al., 2001; Starkel, 2003; Bridgland and Westaway, 2008) have proposed that many river terrace sequences have a combined tectonic–climatic origin. Such river terraces provide information on both tectonic and climatic influences, although challenges arise in identifying their respective roles.

The Kunlun Range (Fig. 1) has experienced both significant late Cenozoic surface uplift (Cui et al., 1998; Wu et al., 2001; Wang et al., 2004b, 2006) and dramatic climatic change (Thompson et al., 1997; Yao et al., 1997) during the late Quaternary. Located at the northern margin of the Tibetan Plateau in Central Asia (Fig. 1A), the Kunlun Range is influenced by both the Asian monsoon and prevailing westerly winds. Modern mountain glaciers are scattered over the Range, which implies that more extensive glacial and periglacial environments likely existed during the last glacial stage (LGS, 75–15 ka; Yao et al., 1997). Numerous late Quaternary terraces are a common feature of rivers along the Kunlun Range, and thus provide a good opportunity for studying the relationship of terrace formation to tectonic and climate forcing factors.

Field work was conducted along four rivers draining the Kunlun Range. Optically stimulated luminescence (OSL) dating was used to establish terrace chronologies. Riverbed and terrace longitudinal profiles of the Kunlun River were measured in the field. The goal

* Corresponding author. Address: Faculty of Earth Sciences, China University of Geosciences, Wuhan 430074, China. Tel.: +86 027 67885099x8405; fax: +86 027 67883002.
E-mail addresses: largeking@sohu.com, anwang@hotmail.com (A. Wang).

1367-9120/$ - see front matter © 2008 Elsevier Ltd. All rights reserved.
doi:10.1016/j.jseaes.2008.09.003

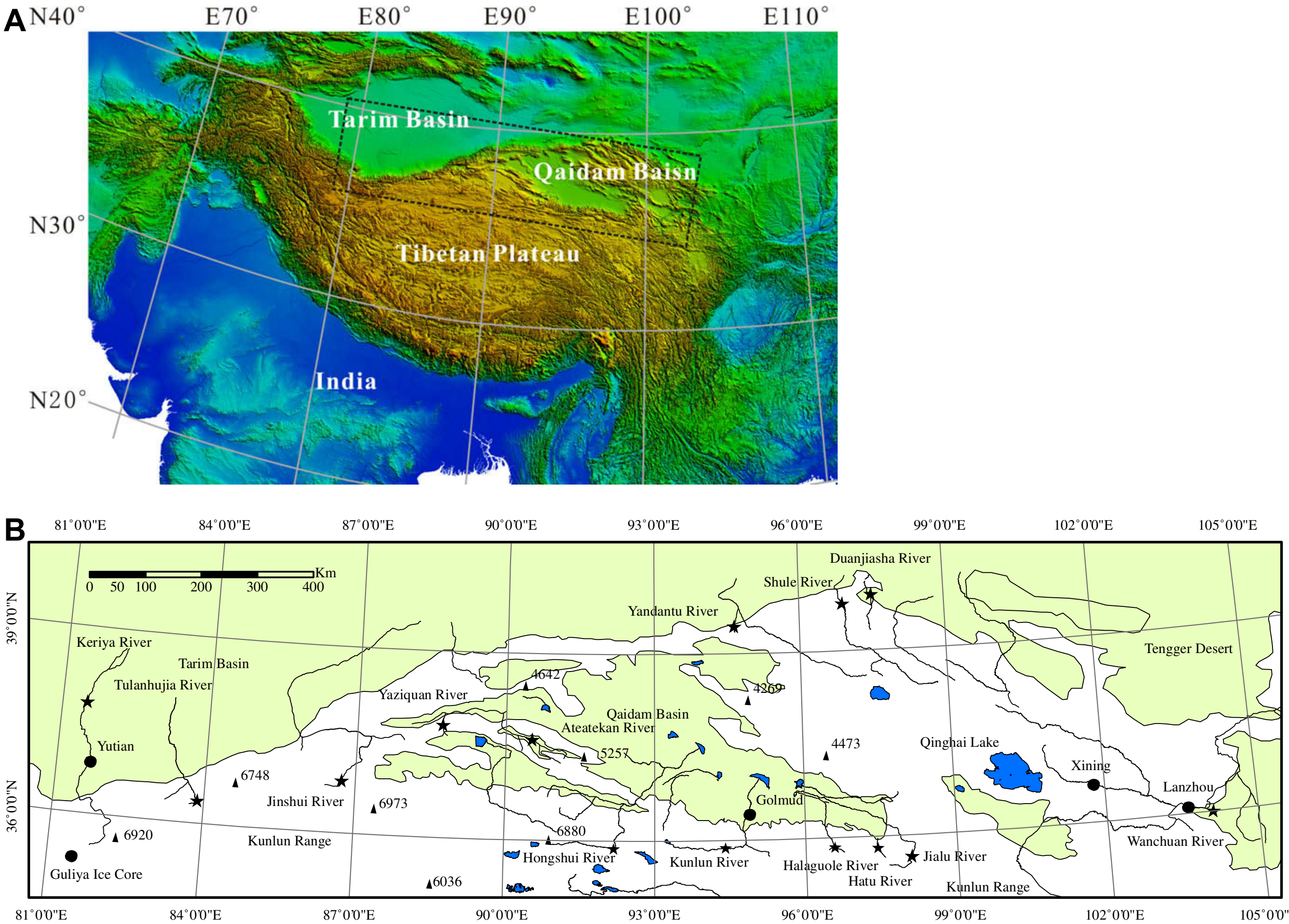

Fig. 1. (A) Digital elevation model of the Tibetan Plateau (Data from SRTM), in which the rectangle indicates the region discussed in the article. (B) A simplified geological and drainage distribution map of the study area. Yellow and blue areas indicate unspecified Quaternary sediments and lakes respectively, filled stars indicate rivers studied in this project, and hollow stars indicate additional rivers discussed in this paper.

was to examine the influence of tectonic and climate factors in terrace formation.

2. Geological background

The Kunlun Range extends approximately 3000 km along the northern margin of the Tibetan Plateau. The highest peak altitudes exceed 7 km (Wang et al., 2005a). The modern climate in the Kunlun area is cold and arid, with an annual temperature of 0–10 °C and mean annual precipitation of 20–300 mm (Zheng, 1999).

The study area (92°00′–97°30′E, 35°40′–36°20′N; Fig. 1) includes four prominent rivers in the eastern Kunlun Range: Kunlun River, Hongshui River, Hatu River, and Halaguole River. The four rivers share broad similarities in geographic setting. They originate from the nearby Range crest, transect the northern slope of the Range, and finally converge in the Qaidam Basin at an altitude of 2800–3000 m. Within the source area for the rivers, peaks above 5300 m are generally capped by glaciers that supply meltwater to these rivers.

As is typical in regions of high topographic relief, the four rivers are characterized by steep gradients, with elevation drops commonly exceeding 1000 m over 100 km. The present vertical uplift rate in the eastern Kunlun Range was estimated by leveling measurements at 7–15 mm/a relative to the Qaidam Basin (Wang et al., 2004b). Significant Pliocene to Quaternary surface uplift was also documented (Cui et al., 1998; Wu et al., 2001; Wang et al., 2006).

3. Methods

3.1. Field work and OSL dating

For the purpose of examining terrace structure and sedimentation, section surveys were carried out on segments with consecutive and laterally continuous terraces. Along each river, terraces were numbered sequentially from the riverbed upward. The numbers thus label a relative chronologic sequence for each river terrace sequence and are useful in identifying local terraces in the field without knowing their absolute ages. As a result, the same terrace numbers between different rivers do not necessarily have concordant absolute ages.

The sampling procedure for OSL dating of terrace and valley fill sediments was as follows:

1. Before sampling, 30–40 cm of surface sediment was removed.
2. Well-sorted fine-sand sediments were located and drilled with metal pipes that could effectively prevent light exposure.
3. Light-tight aluminum foil was used to seal pipe ends to prevent light exposure and water content change during later transportation.

The OSL dating was performed at the State Key Laboratory of Earthquake Dynamics, Institute of Geology in China Earthquake Administration in Beijing. The sample preparation method was based on Lu et al. (1988) and Frechen et al. (1996), in which

<90 μm fractions were extracted by dry-sieving. H_2O_2 (30%) and HCl (37%) were then used to remove organic compounds and carbonates, respectively. Afterwards fine-grained polymineral material (4–11 μm) was obtained by static sedimentation based on Stokes' Law. Aliquots were then made by mounting polymineral suspension dissolved by acetone on stainless steel discs; each aliquot contained ~1 mg of polymineral sample.

Luminescence measurements were carried out on a Daybreak 1100A system. Luminescence signal was stimulated by Post-IRSL (470 ± 5 nm, ~38 mW/cm^2) for 300 s at 125 °C with 10 s preheating at 260 °C. The OSL signal was detected by a photomultiplier tube (EMI QA9235) and two U-340 glass filters. Daybreak 810 beta source (0.0652 Gy/s) was used for irradiation. The equivalent dose was calculated by the first 5 s integral of the OSL decay curve subtracted by the last 5 s.

Equivalent dose was determined using simplified multiple aliquot regenerative-dose protocol (see Wang et al. (2005b) and Lu et al. (2007) for a detailed method description). Generally more than three aliquots were measured for natural OSL intensity, and more than five were used to construct a dose-response curve on which the average natural OSL intensity was projected to yield an equivalent dose.

Approximately, 30 g of fresh material was extracted for water content determination. Uranium and thorium contents were determined by a Daybreak 582 thick source alpha counting and potassium content was determined by flame spectrum analysis. Both errors were estimated within 10%. The elemental concentration and water content were converted into dose rate according to Aitken (1985). The α efficiency was cited as 0.04 ± 0.02 for all samples, based on the study of Rees-Jones (1995). The cosmic-dose rate was corrected by sample altitude and depth based on Prescott and Hutton (1994).

A common concern in applying luminescence dating techniques to sediments is the background luminescence signal, which was confirmed to be significant in insufficient light-exposure environments (Godfrey-Smith et al., 1988; Rendell et al., 1994; Yin et al., 1999). However, for alluvial sediments, feasibility in determining ages has been well-verified by numerous applied and experimental studies (Godfrey-Smith et al., 1988; Rendell et al., 1994; Yin et al., 1999). Experiments indicate that OSL signals in quartz can fall to 1% by sunlight bleaching in 20 s (Godfrey-Smith et al., 1988). In this study, we aimed to avoid partial-bleaching problems by sampling fine-grained and well-sorted sediments that were likely to be well bleached during transport.

3.2. Riverbed and terrace longitudinal profile measurement

According to Hack (1973), graded rivers at dynamic equilibrium, in which riverbed geometry adjusts to changes in discharge and load (Mackin, 1948), can be described by the following formula: $H = C - K \times \ln L$, where H is riverbed altitude, L is river length to source, and C is a constant and K is referred to as gradient index. Actual riverbed longitudinal profiles commonly deviate from this idealized model. The pattern of deviations can be used to analyze the roles of tectonic, climatic, lithologic, and other local factors in river landform building (Hack, 1973; Merritts et al., 1994; Brookfield, 1998). The gradient index for the whole river ($K = \Delta H/\ln L$) is more sensitive to the river's total altitude drop (ΔH) than to its length (Chen et al., 2003). As differential uplift occurs in the drainage area, an increased gradient index (K) is recorded (Fig. 2). The gradient index describes the stream power and allows comparison between rivers of different size (Brookfield, 1998; Chen et al., 2003).

An optical theodolite (TDJ6) and a handset GPS (eTrex Summit) were used to measure the riverbed altitude (absolute height) and terrace elevation (vertical distance above riverbed) profiles of the Kunlun River. Along the upper reach of the Kunlun River, which is characterized by a broad and shallow valley floor, the riverbed longitudinal profile and terrace elevations were measured directly by theodolite and vertical measuring rod. Along the gorges in the lower reach (mainly the Golmud segment), where vertical measuring rods were not useable, altitude and position data (usually on terrace five) were obtained by handheld GPS and terrace elevations were determined by measuring tape. The lengths of river segments between measured points were calculated from GPS data by ARCGIS 9.0 software.

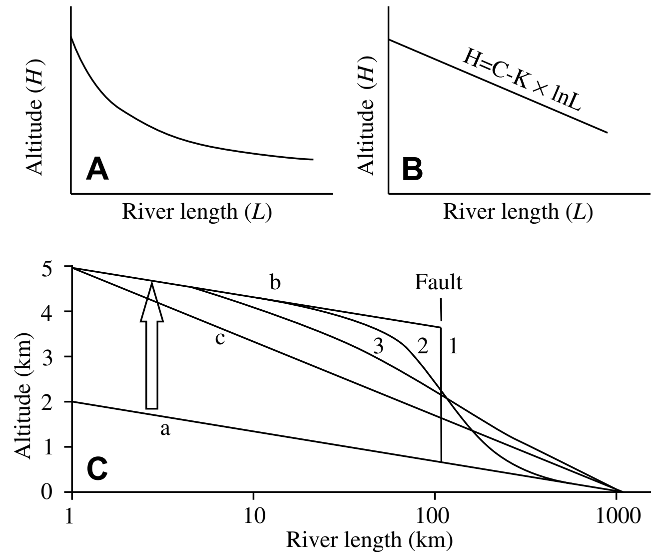

Fig. 2. Linear (A) and semi-logarithmic (B) plots for graded riverbed longitudinal profile and a model (C) showing graded riverbed and its gradient index response to fault movement (uplift). As uplift occurs in the drainage area (indicated by a sudden faulting), the riverbed adjusts (indicated by 1–3) to new graded status (indicated by a–c) with an increase in river gradient index (K) (after Brookfield, 1998).

The vertical and horizontal system errors of the TDJ6 theodolite were 10 angular seconds and 6 angular seconds, respectively. Practical errors were proportional to the measured distance and height. Under normal conditions, maximum vertical errors were less than 2 cm for a 50-m high terrace measured over a 300 m distance, while horizontal errors were even smaller. These errors indicate high precision for terrace and riverbed measurements. The handheld GPS equipped with a barometer had a vertical error of 2.5 m. To minimize the internal error, measurements were performed under clear climatic conditions without any dramatic weather changes.

4. Results

4.1. Kunlun River

The Kunlun River consists of three segments: the NS-oriented Xiaonanchuan segment, the EW-oriented Nachitai segment, and the NS-oriented Golmud segment, each of which has a distinctive valley landscape (Fig. 3). The Xiaonanchuan segment is an upper tributary of the Kunlun River, most of which is characterized by a broad and shallow valley floor. Terrace elevation shows a gradual increase downstream. Continuous, high terraces emerge only at the northern part. The Nachitai segment, which is also characterized by a broad and shallow valley floor, has numerous well-developed terraces with lateral continuity over dozens of kilometers. The best-developed terraces are located at Sanchakou (Fig. 3B) in the western part of the Nachitai segment (Wu et al., 2001; Wang et al., 2003; Owen et al., 2006), where five terraces occur. Directly upstream of the Golmud segment, the river channel narrows and lower terraces disappear, and the Golmud segment is characterized by a deeply incised gorge (Fig. 3C). However, the uppermost ter-

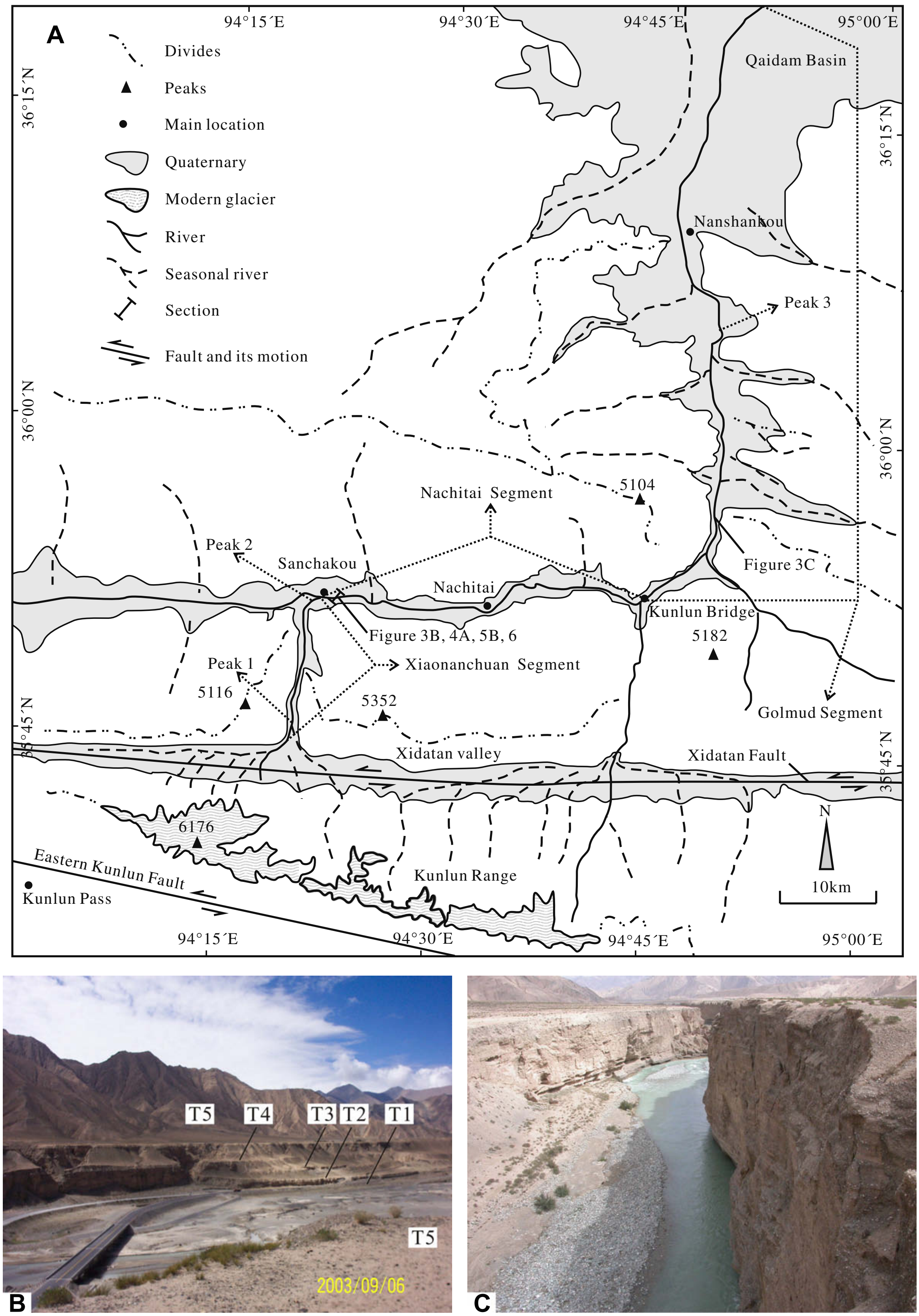

Fig. 3. (A) Simplified geologic and geographic map for Kunlun River which is divided into three segments. Terrace elevation peaks labeled are for discussion in Section 4.4. (B) Five well-developed terraces at Sanchakou, where the Nachitai segment is characterized by a broad, shallow channel. The uppermost terrace (T5), which constitutes the main valley fill, has the best lateral continuity and can be traced along the whole river system. The lowermost terrace (T1) constitutes the base of the road on the far bank where a truck can be seen. View is to the southwest. (C) Typical gorge in the Golmud segment where only T5 is widely preserved. The T5 elevation in the figure is ~30 m. view is to the north.

race (T5) continues along almost the entire length of the Kunlun River (Owen et al., 2006).

The present Kunlun River channel and numerous terraces are incised into an unconsolidated late Quaternary sediment sequence (Wu et al., 2001; Wang et al., 2003), which makes up the valley fill (Fig. 4A). A typical valley fill sequence was examined at the start of the Nachitai segment (Fig. 5A). The 47.3 m thick valley fill consists primarily of layers of clast-supported gravel with minor interbedded sands and silts (Wu et al., 2001; Owen et al., 2006). Lenticular sands are a common feature. The characteristics of the valley fill sediments suggest a braided river environment with a high sediment load (Cui et al., 1999; Wu et al., 2001). OSL dating of sandy sediments embedded in this sequence yielded ages of 16.6 ± 2.2 ka at the top and 90.1 ± 10.0 ka at the bottom (Table 1).

Each terrace, from lowest (T1) to highest (T5), has its own sediment package, typically characterized by channel facies of gravels with an imbricate structure. A secondary facies is commonly present as well. For example, T2 consisted of channel facies overlain by overbank facies of layered sand and silt (Fig. 6) with an OSL age of 8.8 ± 1.0 ka (Table 1). A previous study obtained OSL ages of 23.87 ± 2.28 ka for the top of T5, and 12.9 ± 1.3 ka and 13.27 ± 0.65 ka for T3 (Wang et al., 2003).

4.2. Hongshui River

The Hongshui River (Fig. 1B), which is located at the western part of the eastern Kunlun Range, flows eastward in a fault valley of the eastern Kunlun Fault (Li et al., 2005) before crossing the Range. Within this fault valley, at least four terraces are well developed in the unconsolidated valley fill (Fig. 4B). A 51.7 m thick valley fill sequence (Fig. 5B) consists mainly of angular clast-supported gravel with layers and lenses of sand. The sedimentary characteristics are consistent with a braided river environment with high sediment load. Based on lithology and imbricate structure, the gravels originated from adjacent sub-valleys. Measurement of the gravel imbricate structure (Fig. 5B) yielded an average trend of 199° near a NS-oriented tributary for the main valley fill. OSL dating yielded bottom ages of 71.3 ± 7.5 ka and 62.7 ± 8.8 ka, and a top age of 19.7 ± 2.2 ka for this sequence (T4); T3 yielded an age of 9.9 ± 1.1 ka (Fig. 4B, Table 1).

4.3. Hatu and Halaguole Rivers

The Hatu and Halaguole Rivers (Fig. 1B) are located in the eastern part of the eastern Kunlun Range. They have a similar terrace structure to the Kunlun and Hongshui Rivers and the valley fill consists of braided river facies. The majority of the Hatu River is confined within the northern slope of the Range. Five well-developed

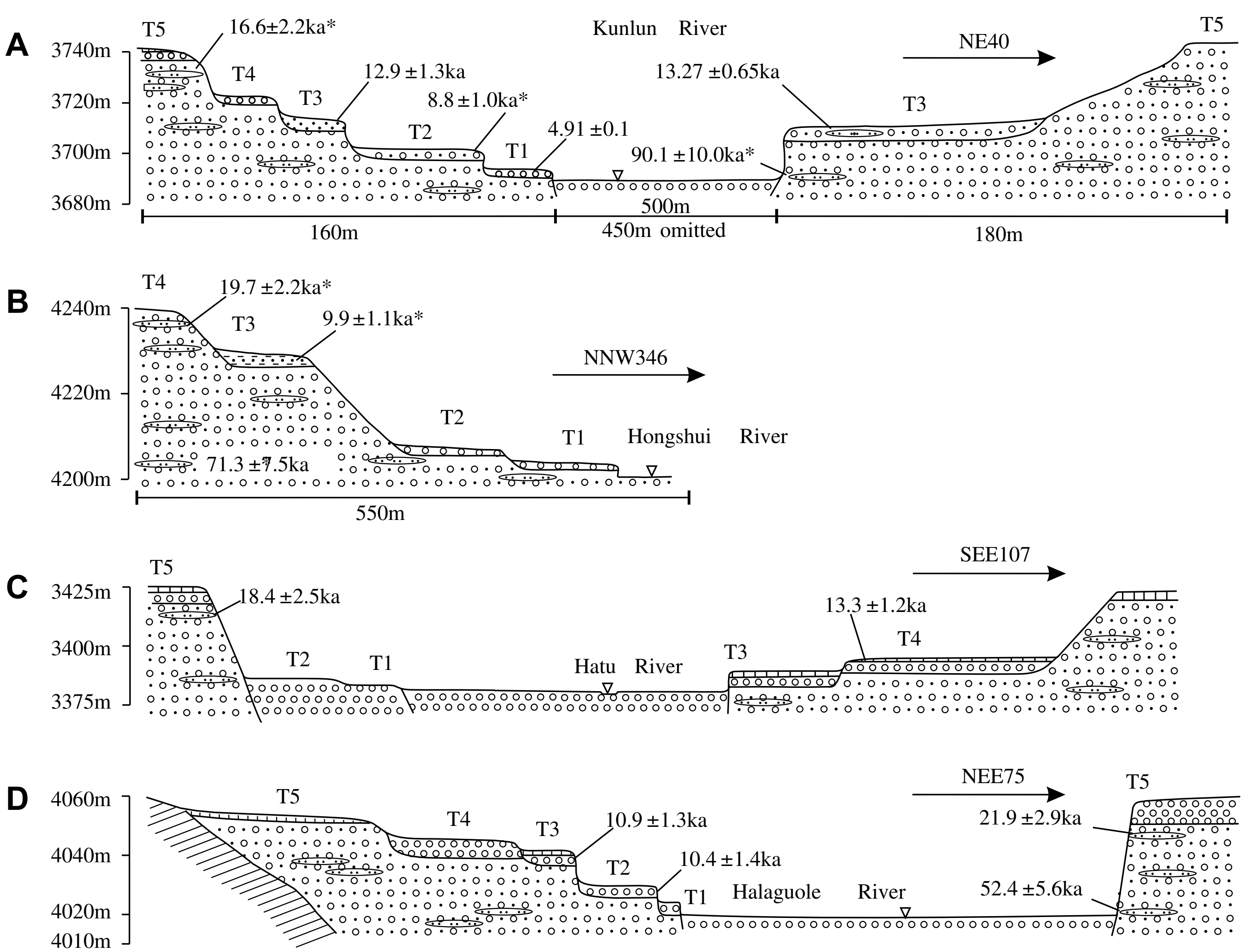

Fig. 4. Sketch map of terrace structures. (A) Kunlun River (35°53.42′N, 94°23.52′E, 3690 m asl). (B) Hongshui River (35°52.58′N, 92°12.43′E, 4204 m asl). (C) Hatu River (35°52.88′N, 97°24.21′E, 3384 m asl). (D) Halaguole River (35°48.36′N, 96°42.44′E, 4022 m asl). Section trend is indicated by arrows. Data obtained in this paper are indicated by an asterisk (*).

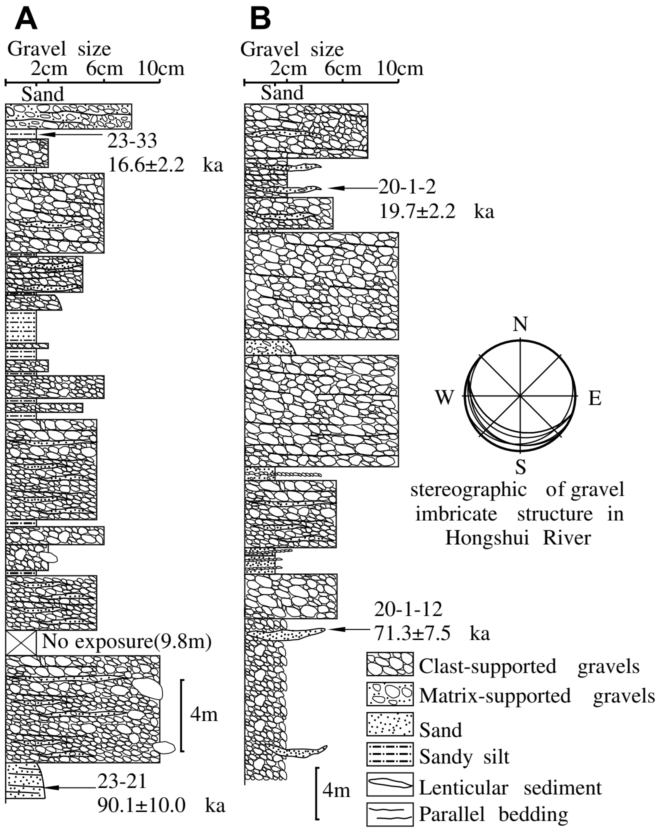

Fig. 5. Stratigraphic columns of valley fill sequences. (A) Kunlun River valley at Sanchakou (35°53.42′N, 94°23.52′E, 3690 m asl). (B) Hongshui River valley (35°52.58′N, 92°12.43′E, 4204 m asl); gravel imbricate structure in this sequence is plotted in stereographic projection.

terraces were identified in the upper reach of the river, of which four terraces are incised into the unconsolidated valley fill with a maximum depth of about 50 m (Fig. 4C). Previous OSL dating yielded an age of 18.4 ± 2.5 ka at the top of the uppermost terrace (Wang et al., 2003). The T4 sediment package, which has a binary structure of gravel layers overlain by silt-sand layers with horizontal bedding, yielded an age of 13.3 ± 1.2 ka (Wang et al., 2003). In the Halaguole River (Fig. 4D), OSL dating yielded an age span of 52.4 ± 5.6 ka to 21.9 ± 2.9 ka for a similar 50 m thick valley fill sequence, and 10.4 ± 1.4 ka for T3, 10.9 ± 1.3 ka for T4, respectively (Wang et al., 2003).

4.4. Riverbed and terrace longitudinal profiles of the Kunlun River

An upward deviation of the riverbed from its ideal graded status can be observed for the Kunlun River (Fig. 7). The gradient index was 130 within an entire river length of about 120 km, from the measured source at an altitude of 4380 m to the river mouth at

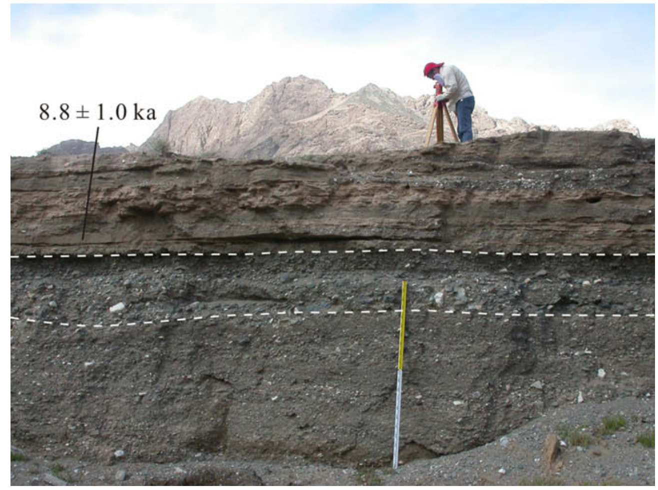

Fig. 6. Binary facies of the T2 terrace of the Kunlun River. The channel facies of the T2 sediment package is indicated by imbricate gravel layers with larger marble pebbles at the bottom (indicated by dashed lines), which is overlain by layered silt, sand, and fine gravel sediments of overbank facies with an OSL age of 8.8 ± 1.0 ka. The scale ruler is 2 m in height. View is to the north.

2858 m. The Xiaonanchuan segment is a tributary of the Kunlun River and a similar gradient index of 129 was obtained for a river length of 205 km and an altitude of 4432 m at the source. The river source altitude and river length were obtained from a 1:100,000 topographic map by ARCGIS 9.0.

Terrace elevations were measured along the length of the Kunlun River (Fig. 7). Five terraces with good lateral continuity are present from the Xiaonanchuan segment to the Nachitai segment of the Kunlun River, whereas only the uppermost terrace (T5) extends into the narrow and deeply incised Golmud segment. Measurements indicate that three peaks (labeled as Peak 1–3; Fig. 3A) in the elevation of T5 are present along the river. The smallest peak (Peak 1: <10 m) is located in the upper reach of the Xiaonanchuan segment at the mouth of a tributary valley; a similar phenomenon was observed by Owen et al. (2006). The largest peak in T5 elevation (Peak 2: ca. 60 m) occurs at the downstream end of the Xiaonanchuan segment near Sanchakou. Numerous succeeding terraces (T4–T1) downstream from Peak 2 also show a concordant trend in terrace elevation (Fig. 7). The northernmost peak in T5 elevation (Peak 3: ca. 50 m) is in the middle of the Golmud segment. Toward both river source and mouth, the surface of T5 converges with the present riverbed.

5. Discussion

5.1. Roles of surface uplift and climatic change in terrace formation

This project focuses on the question of whether surface uplift or climatic change was the principal factor in the incision of valley fill

Table 1
OSL dating results for terraces of the Kunlun River and Hongshui River

Sample number	Terrace	Depth (m)	H_2O (%)	α-count (/Ksec)	K_2O (%)	Dose rate (Gy/ka)	Equivalent dose (Gy)	Age (ka)
23-21	Kunlun-T5	40.0	2	9.0±0.2	2.0	3.6±0.3	327.1±16.4	90.1±10.0
23-28	Kunlun-T2	0.8	1	8.9±0.2	2.5	4.2±0.4	37.5±1.6	8.8±1.0
23-33	Kunlun-T5	8.0	1	9.5±0.3	2.2	4.1±0.4	65.9±6.0	16.6±2.2
20-1-2	Hongshui-T4	4.8	8	7.3±0.2	1.8	3.1±0.2	60.0±3.5	19.7±2.2
20-1-12	Hongshui-T4	39.8	1	6.7±0.2	1.6	2.8±0.2	201.8±6.8	71.3±7.5
20-3	Hongshui-T3	0.6	4	9.3±0.2	2.3	3.9±0.3	40.3±2.2	9.9±1.1
1565	Hongshui-T4	35	4	9.8±0.2	2.3	4.1±0.4	256.2±25.2	62.7±8.8

Sample processing was carried out at the State Key Laboratory of Earthquake Dynamics, Institute of Geology, China Earthquake Administration. Alpha efficiency was estimated as 0.04 ± 0.02 for all samples.

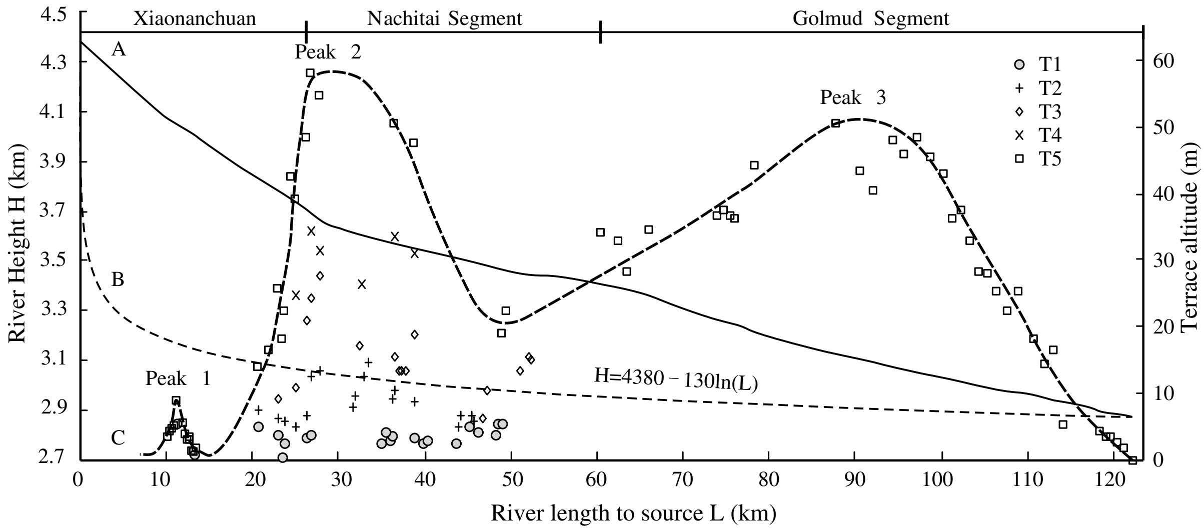

Fig. 7. Actual riverbed (A: plotted on the left axis), ideal graded riverbed (B: plotted on the left axis), and terrace elevation measured along longitudinal profile (C: plotted on the right axis) of the Kunlun River. Terrace elevation is vertical distance above the local riverbed.

and formation of numerous terraces. As indicated by the riverbed longitudinal profile (Fig. 7), the modern Kunlun River riverbed deviates upward from its ideal graded profile over the scale of the entire drainage. Based on studies in Taiwan Island, Chen et al. (2003) suggested that drainage-scaled deviation of the riverbed from a graded profile is caused by large-scale tectonic activity. This idea is supported by the considerable late Cenozoic surface uplift that has occurred in the drainage area of the Kunlun Range (Cui et al., 1998; Wu et al., 2001; Wang et al., 2004b, 2006). As a feedback, incision should have initiated and strengthened as the surface uplift progressed. However, uplift-induced incision itself cannot account for the regional aggradation of valley fills during the LGS (75–15 ka) and the subsequent aggradational episodes of mantled terrace-sediment packages (Maddy et al., 2001). As the

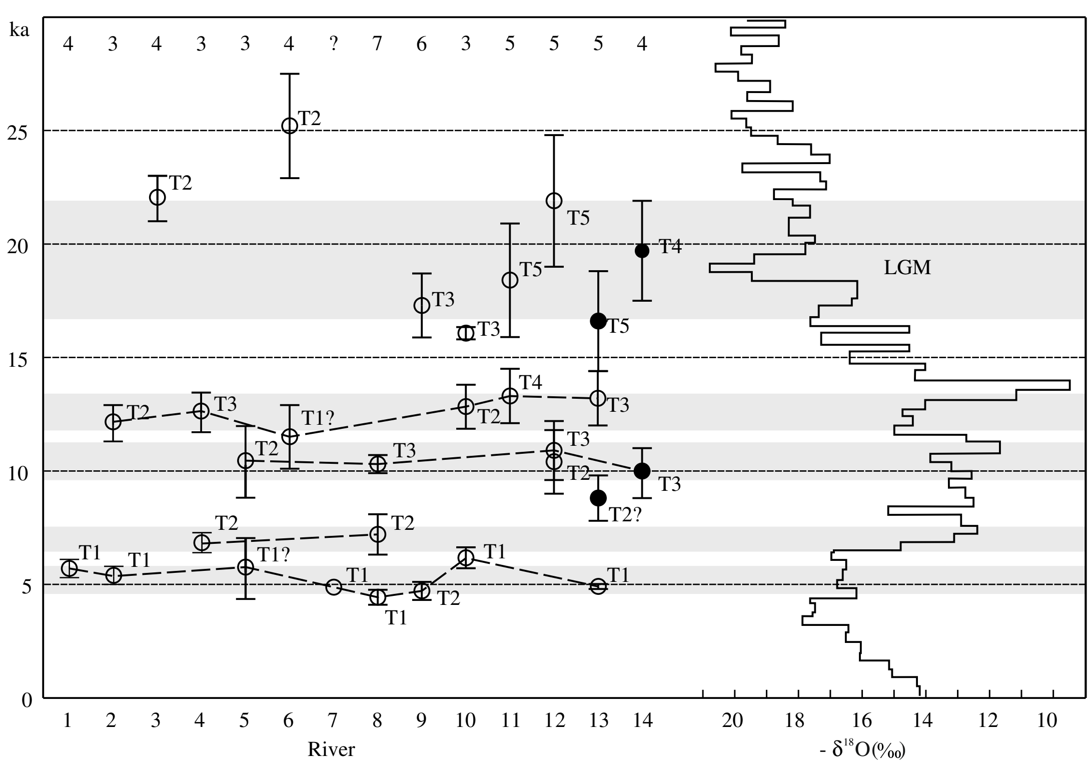

Fig. 8. Age sequences for terraces along rivers in northern Tibet and the climatic proxy record of $\delta^{18}O$ from the Guliya ice core (35°17′N, 81°29′E; after Thompson et al., 1997). The total number of terraces for each river is marked on top of each series. Solid circles indicate newly obtained data listed in Table 1. Hollow circles indicate data from various sources, in which all terraces with ages between 30 ka and 4 ka are included. Shaded areas indicate clustered intervals of mean value (±2σ) for each group. 1. Jialu River (Li et al., 1997); 2. Tulanhujia River (Zhao and Li, 2006); 3. Jinshui River (Zhao and Li, 2006); 4. Ateatekan River (Zhao and Li, 2006); 5. Yaziquan River (Zhao and Li, 2006); 6. Duanjiasha River (Wang et al., 2004a); 7. Wanchuan River (Wu and Yang, 2006); 8. Shule River (Wang et al., 2004a); 9. Keriya River (Wang et al., 2004c); 10. Yandantu River (Zheng et al., 2004); 11. Hatu River (Wang et al., 2003); 12. Halaguole River (Wang et al., 2003); 13. Kunlun River (Wang et al., 2003; Wang and Bian, 1993); 14. Hongshui River.

chronological data indicate, the abrupt switch from regional aggradation to incision in the valley occurred after 21.9 ± 2.7 ka to 16.6 ± 2.2 ka, which coincided with the global last glacial maximum (LGM; ca. 21 ka). This timing is consistent with the classic framework of cold-stage aggradation and warming-stage incision (Seddon and Holyoak, 1985; Bridgland, 2000; Maddy et al., 2001; Colin, 2002; Starkel, 2003; Vandenberghe, 2003). It is thus suggested that the post-glacial climate modulated the valley incision and subsequent terraces (Van der Woerd et al., 1998). Terrace elevation diminishes as the Kunlun River enters the Qaidam Basin, which indicates that terrace incision was not initiated upstream by a base-level decrease.

The overall conclusion is that the surface uplift provided a potential driving force for incision, while climatic change provided the trigger for aggradation and incision. To further explore this correlation, terrace ages from a wider region were assembled for comparison with climatic records.

5.2. Regional terracing sequences

We analyzed additional terrace ages that fell within the time range of the four rivers we studied (30–4 ka). It should be noted that we did not independently evaluate the reliability of the collected terrace ages, and that such an evaluation is not part of the statistical analyses. We performed cluster analysis (Appendix A) and calculated the mean square of weighted deviates (MSWD) for the entire data set. The resulting terrace age results are presented as 2σ confidence intervals with cluster ages and MSWD in parentheses.

Cluster analysis of chronological data from 14 rivers with a total of 30 terraces identified at least four major regional terrace aggradational periods: 13.4–11.8 ka (12.6 ± 0.8, 0.33), 11.0–9.6 ka (10.3 ± 0.7 ka, 0.12), 7.7–6.1 ka (6.9 ± 0.8, 0.13), and 5.8–4.6 ka (5.2 ± 0.6, 2.49) (Fig. 8). Terrace numbers (e.g., T1 and T2), which mark relative chronological sequences within single terrace sequences, are typically inconsistent between individual rivers, so correlation of terrace chronologies between different river systems was used as the primary means of identifying terracing periods.

Interpretation of terrace sequences from regional terrace chronologies enables construction of a more complete terracing history, which can be better correlated to climate history. However, uncertainty may arise in clustering data with lower precision (indicated by question marks in Fig. 8). Evidence for additional terracing periods (e.g., T4 and T2 of Kunlun River) could emerge if more comprehensive chronologies become available.

5.3. Aggradation and incision driven by climatic change

In recent climatic studies of Tibet, considerable attention has been focused on the abnormally high precipitation during the LGS. Several wet intervals (pan-lake periods) during the LGS in northern Tibet have been identified [e.g., 65–53 ka (Zheng et al., 2006), 40–30 ka (Hans-Joachim et al., 1995; Zheng et al., 2000, 2006; Jia et al., 2001; Shi et al., 2001)]. Enhanced Indian monsoon precipitation was likely two to five times greater than at present between 40 and 30 ka (Pachur et al., 1995; Jia et al., 2001). A combination of high sediment availability and increased precipitation can result in substantial aggradation of the valley floor (Maddy et al., 2001). Abundant precipitation during the LGS is hypothesized to be a probable climatic trigger for the regional valley aggradation in the study area. This hypothesis is consistent with the sedimentary environment of the valley fill (high sediment load), and the observation that the sediments were characteristically contributed by sub-valleys.

The transition from aggradation to incision that occurred during marine isotope stage (MIS) 2 may have been caused in large part by precipitation starvation. Evidence that the maximum glacial advance in northern Tibet occurred in MIS3 (Finkel et al., 2003; Shi and Yao, 2006), even though temperatures were lower in MIS2 (Yao et al., 1997), implies that precipitation was limited in MIS2. The timing of the transition suggests that in the hyperarid Kunlun Range of northern Tibet, effective precipitation might be more important than temperature in causing environmental change (Shi et al., 2002). The progressive incision that succeeded the large-scale aggradation was consistent with the overall aridity trend since MIS3. Contemporaneous lake sedimentation evolution in the Qaidam Basin indicates that freshwater deposition of clastics and shells occurred between 40–30 ka and that desiccation was prevalent from 25–9 ka (Chen and Bowler, 1986). In Tengger Desert in northwestern China, widespread fresh-mesohaline paleolakes occurred between 42–20 ka and completely disappeared at 18 ka (Pachur et al., 1995; Zhang et al., 2002).

As a proxy for past climatic change, the oxygen isotope curve from the Guliya ice cap (Thompson et al., 1997; Yao et al., 1997) in the western Kunlun Range provides a unique opportunity for examining the relationship between terracing periods and climatic change (Fig. 8).

The 13.4–11.8 ka terracing period is correlated to a cooling transition at approximately 14–12 ka in the Guliya ice core, which shows a significant decreasing trend in $\delta^{18}O$ value (Thompson et al., 1997; Yao et al., 1997). Recent glacial studies in Tianshan (northwestern Tibet) revealed a glacial advance with a cosmogenic radionuclide age of 12.4 ka (Kong et al., 2006). A late glaciation

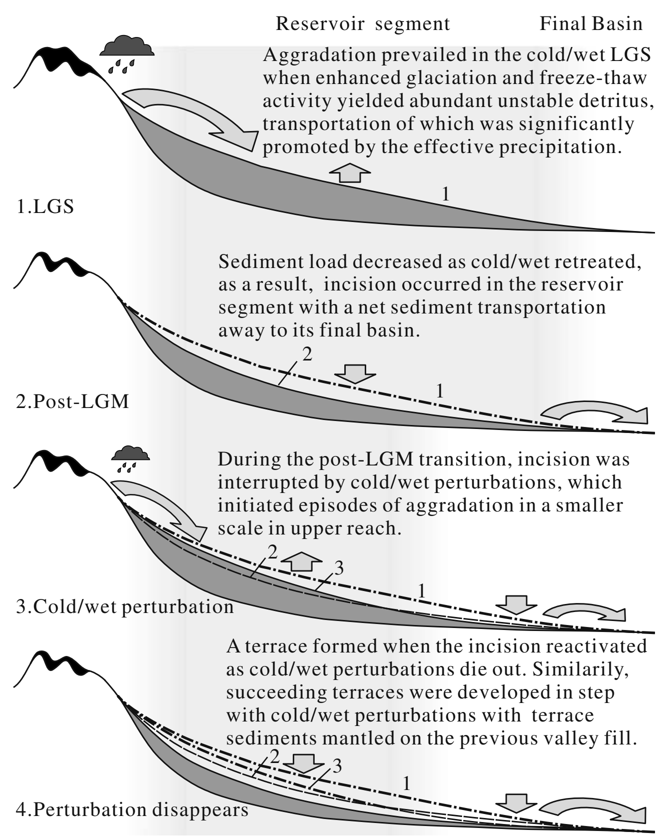

Fig. 9. A model for river terrace evolution triggered by climate change in a mountain range that has undergone considerable surface uplift. Curved arrows indicate the net sediment transport for the reservoir segment marked by the shaded area, the scale of which is qualitatively indicated by the size of the shaded area and the arrow. Vertical arrows and numbered lines indicate vertical adjustments of the riverbed, which thus produce terraces. Dot-dashed lines indicate terrace surfaces, of which the uppermost terrace is indicated by 1 and the next lower terrace in the upper reach is indicated by 3.

(13.4–12.6 ka) was identified in northern Tibet based on a variety of calibrated ^{14}C ages (Yi et al., 2006). Lake core records in northern Tibet suggest that relatively abundant precipitation accompanied this cooling perturbation (Li et al., 1994; Hu et al., 2002). A wet period was also recorded in the Qinghai Lake sediments (13.7–12.9 ka; Shen et al., 2005), the loess sediments (13.3–11.8 ka; An et al., 1993) in northeastern Tibet, and paleolake terraces (12.8 ka) in Tengger Desert (Pachur et al., 1995).

The 11.0–9.6 ka terracing period may correspond to a late glacial cooling in the Guliya ice core oxygen isotope curve, although the cooling interval in the curve is minor. Lake core records in northern Tibet suggest that the climate was cold and wet between 10.4 and 9.8 ka (Hu et al., 2002). A consistently wet climate was also recorded in the Qinghai Lake sediments between 12.1 and 9.8 ka (Shen et al., 2005). Glacial studies in western Tibet (Owen et al., 2002) revealed a glacial advance with a cosmogenic radionuclide age of 10.9–9.0 ka, which was attributed to a precipitation change combined with cooling. The isolated age of 8.8 ± 1.0 ka of T2 in the Kunlun River may be correlated to cooling at 9.4 ka or 8.2 ka (Wang et al., 2002) in the early Holocene.

The 7.7–6.1 ka and 5.8–4.6 ka terracing periods correspond to the transition from the early Holocene climatic optimum to the Neoglacial stage, which has been interpreted as a period of abundant precipitation (Shi et al., 2002). Jia et al. (2001) suggested that lakes on the Tibetan Plateau expanded to 180% of their present area during the interval 9.0–5.0 ka as a result of enhanced monsoon precipitation. Early- to mid-Holocene wet conditions were also recorded in Qinghai Lake (Shen et al., 2005).

The correlation of terracing periods and climatic fluctuations strongly suggests that the terrace aggradations were related to cooling and/or wet perturbations in the climate. Temperature change affects terrace-building through its indirect control on the sediment supply, which increases during cooling stages as glaciers expand and freeze-thaw activity intensifies, then decreases during warming stages as glaciers retreat and freeze-thaw activity diminishes (Bull, 1991; Maddy et al., 2001). Temperature-related terracing has been observed by Maddy et al. (2001) in the Thames Valley of the UK and by Starkel (2003) in central Europe, where terrace sediment packages commonly developed during cold stages and large-scale incision that formed terraces initiated at the warming limbs of major glacial–interglacial cycles. Moreover, the terrace sequences in the arid Kunlun Range suggest that precipitation was an indispensable factor in terrace-building. The role of precipitation in terrace-building is most likely to facilitate effective transportation of detritus from around the drainage basin to the valley floor, which could create a significant aggradational episode during progressive incision. However, as was suggested by Bridgland and Westaway (2008), studies rarely distinguish the respective roles of temperature and precipitation.

5.4. A model for river terrace formation

The three peaks in terrace elevation along the Kunlun River (Fig. 3A) can be thought of as sediment reservoirs. Peak 2 at the downstream end of the Xiaonanchuan segment was evidently constructed by sediment transportation to the Nachitai segment from the Xidatan valley, where numerous alluvial fans were developed by outwash from modern glaciers originating in the main ridge. The NS-oriented Xiaonanchuan valley (Fig. 3A) served as a reservoir for storage and transportation of sediments northward from the Xidatan Valley to the Kunlun River valley. The confluence with the Kunlun River was analogous to a floodgate, where sediments were released into the Kunlun River valley. Similarly, Peak 3 in the Golmud segment corresponded to another reservoir in the

Table 2
Regional terrace ages in northern Tibet collected for cluster analysis, in which all data between 30 and 4 ka are included

River	Method	Terrace number	Elevation (m)	Age (ka)	Source
Duanjiasha River	OSL	T1	6.0	11.5 ± 1.4	Wang et al. (2004a)
	OSL	T2	14.5	25.2 ± 2.3	
Shule River	OSL	T1	8.6	4.43 ± 0.33	
	OSL	T2	21.5	7.2 ± 0.89	
	OSL	T3	33.9	10.3 ± 0.4	
Keriya River	OSL	T2	20.0	4.71 ± 0.4	Wang et al. (2004c)
	OSL	T3	31.5	17.29 ± 1.41	
Wanchuan River	^{14}C	T1	20. 0	4.87 ± ?	Wu and Yang (2006)
Yandantu River	TL	T1	19.0	6.17 ± 0.46	Zheng et al. (2004)
	TL	T2	61.0	12.83 ± 0.97	
	TL	T3	73.0	16.07 ± 0.27	
Hatu River	OSL	T4	14.0	13.3 ± 1.2	Wang et al. (2003)
	OSL	T5	43.0	18.4 ± 2.5	
Halaguole River	OSL	T2	6.0	10.4 ± 1.4	
	OSL	T3	21.0	10.9 ± 1.3	
	OSL	T5	42.0	21.9 ± 2.9	
Kunlun River	^{14}C Cosmogenic dating	T1	3.0	4.91 ± 0.11 (5.106 ± 0.29)	Wang and Bian (1993) and Van der Woerd et al. (1998)
	OSL	T2	8.1	8.8 ± 1.0(8.8 ± 0.8 ka)	This paper Owen et al. (2006)
	OSL	T3	15.4	13.2 ± 1.2	Wang et al. (2003)
	OSL	T5	51.0	16.6 ± 2.2	This paper
Hongshui River	OSL	T3	37. 0	9.9 ± 1.1	
	OSL	T5	50.0	19.7 ± 2.2	
Jialu River	TL	T1	4.0	5.7 ± 0.4	Li et al. (1997)
Ateatekan River	TL	T2	8.4	6.84 ± 0.44	Zhao and Li (2006)
	TL	T3	22.4	12.58 ± 0.87	
Jinshui River	OSL	T2	40.0	22.0 ± 1.0	
Tulanhujia River	OSL	T1	17.5	5.4 ± 0.4	
	OSL	T2	38.0	12.1 ± 0.8	
Yaziquan River	OSL	T1	15.0	5.7 ± 1.34	
	OSL	T2	25.0	10.4 ± 1.58	

Note: Data in brackets indicate determined from the same terrace in a river, which do not participate in cluster analysis for the purpose of allowing an equal weight between rivers.

landscape with its floodgate set at Nanshankou, from which downstream terrace elevation dropped quickly. Sediments were supplied to the peak region by a series of tributaries from Kunlun Bridge to Nanshankou (Fig. 3A). Within the Golmud segment, the main river channel was shifted away from tributary mouths (Fig. 3A), which suggests that during high sediment load periods, valley aggradation tended to occur predominantly in the reservoir segment and the stream passively adjusted to the high sediment injection by sub-tributaries. Beyond Nanshankou, terrace elevation decreases and finally converges with the present riverbed and the base of the Qaidam Basin.

A reservoir segment in a river acts alternately as a space for localized sediment accumulation during periods of high sediment load, and as a site of sediment transportation to the final basin during periods of low sediment load. Aggradation and incision alternate in the reservoir segment as high sediment load perturbations emerge and then fade away, which can be caused by enhanced glaciation and freeze-thaw activity during cold stages (Bridgland, 2000; Maddy et al., 2001; Colin, 2002; Starkel, 2003). Relatively abundant precipitation promotes the transportation of detritus over the drainage basin to nearby valley floors. Numerous terraces are thus formed in a reservoir segment by alternation between episodes of aggradation and incision (Fig. 9).

Aggradation and incision occur at different temporal and/or spatial scales, depending on the scale of climatic change (Fig. 9). For example, in the Kunlun Range, regional aggradation prevailed during most of the LGS and formed valley fill sequences more than 50-m thick, whereas terrace-related aggradation occurred as episodes during the progressive incision since the LGM and was more confined within the upper reaches. The limited extent of terrace-related aggradation indicates a temporal and spatial scale of climatic change that was smaller than the climatic change responsible for the valley fill. A significant shrinkage of the spatial scale of aggradation from the deposition of the valley fill to the development of the succeeding terraces can account for the difference in the river landscape between the upper reach, where numerous episodic terrace aggradations were developed, to the lower reach, which is characterized by narrow gorges and has been undergoing constant incision since the LGM.

6. Conclusions

Along the Kunlun Range in northern Tibet, comparable Late Pleistocene valley fill sequences were identified in several river valleys. The related regional aggradation period was OSL-dated to be mainly within the LGS (75–15 ka; Yao et al., 1997). The succeeding terraces with common incision depths of 50–60 m within the valley fill sequence were OSL-dated to be post-LGM (<ca. 15 ka), when the valley aggradation ceased and the uppermost terraces developed. Based on a broad range of terrace chronologies in northern Tibet, four synchronized terracing periods were recognized: 13.4–11.8 ka, 11.0–9.6 ka, 7.7–6.1 ka, and 5.8–4.6 ka. The correlation between the timing of terracing periods and climatic shifts indicated by various proxy records suggests that terrace formation was triggered by cooling and/or wet perturbations in the climate. The significant late Cenozoic surface uplift tended to exert a long-term driving force for riverbed incision.

Based on valley aggradation characteristics, terrace chronologies, and the riverbed and terrace longitudinal profile data, a simplified model is proposed. The model correlates climatic factors to river terrace aggradation and incision, and also accounts for the differential development of river terraces between different reaches.

This study indicates that climatic factors (mainly temperature and precipitation) were significant in shaping landforms in the hyperarid Kunlun Range. River terrace systems in the Kunlun Range are an excellent archive for past climatic changes in northern Tibet, especially for major cooling and/or wet perturbations during the post-LGM period. The timing of the 13.4–11.8 ka terracing period suggests that it may be related to the Younger Dryas climate reversal. Special care should be taken in using sediments as evidence for instantaneous plateau uplift alone, as the climatic effect may be significant. With further work over a wider region of river terrace systems in this area and development of detailed terrace chronologies, it should be possible to develop a more complete climatic history and provide further insights into the respective roles of temperature and precipitation in terrace-building.

Acknowledgements

This study was financially supported by the China Geological Survey Institute (No. 1212010610103, No. 200313000005) and the National Natural Science Foundation of China (No. 40672137). We are grateful to Dewei Li, Qirong Wei, Xiongfei Cai, as field work was greatly assisted by them. Appreciation also goes

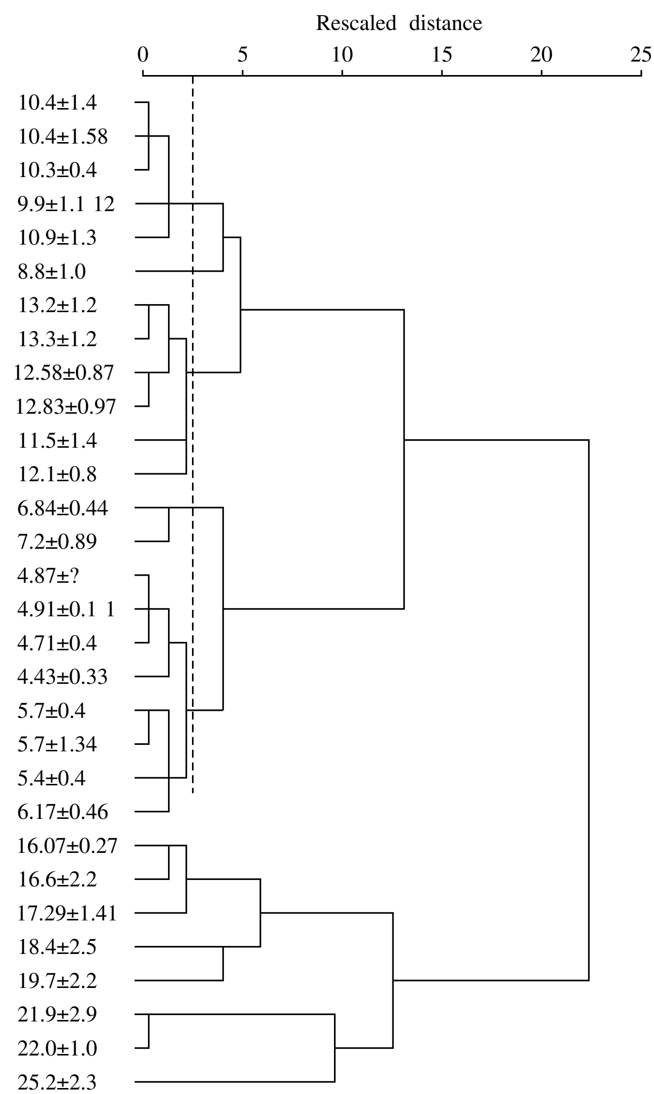

Fig. 10. A dendrogram for the hierarchical cluster analysis of data collected in Table 2. A threshold distance in classifying terracing periods is indicated by a dashed line, based on a combination with terrace number information.

to Julia Ellis Burnet and John I. Garver, who improved earlier version of this paper. The authors express special appreciation to Lewis Owen, Yue-Gau Chen, and an anonymous reviewer for their detailed and constructive reviews and helpful suggestions.

Appendix A. Cluster analysis

The aim of this cluster analysis is to find possible relationships among terrace ages of different river system. Duplicated chronologies in the same river were avoided in cluster analysis to allow an equal weight between river systems. The hierarchical clustering method was employed, in which the following steps are followed for terrace chronologies collected in Table 2:

1. Define $\overline{A_i}$ as average age of a cluster/element *i*.
2. Define simple euclidean distance as $D_{ij} = |\overline{A_i} - \overline{A_j}|$ between cluster/element *i* and *j*.
3. At the beginning each age element is considered as a cluster, and simple euclidean distance between each element is calculated.
4. Cluster the two elements with a minimum distance and then calculate new distance between each element and cluster.
5. Repeat step 4 until all elements are included into a final cluster, and a dendrogram is constructed (Fig. 10).
6. The cluster number is determined by a distance threshold. Taking into account practical terrace number, these terrace ages can be best classified into five major clusters which are indicated by shaded belts in Fig. 8.

References

Aitken, M.J., 1985. Thermoluminescence Dating. Academic Press, London. p. 395.

An, Z., Porter, S.C., Zhou, W., Lu, Y., Donahue, D.J., Head, M.J., Wu, X., Ren, J., Zheng, H., 1993. Episode of strengthened summer monsoon climate of Younger Dryas age on the Loess Plateau of Central China. Quaternary Research 39, 45–54.

Bridgland, D., Westaway, R., 2008. Climatically controlled river terrace staircases: A worldwide Quaternary phenomenon. Geomorphology 98, 285–315.

Bridgland, D.R., 2000. River terrace systems in north–west Europe: an archive of environmental change, uplift and early human occupation. Quaternary Science Reviews 19, 1293–1303.

Brookfield, M.E., 1998. The evolution of the great river systems of southern Asia during the Cenozoic India-Asia collision: rivers draining southwards. Geomorphology 22, 285–312.

Brunnacker, K., Löscher, M., Tillmans, W., Urban, B., 1982. Correlation of the Quaternary terrace sequence in the lower Rhine valley and northern Alpine foothills of central Europe. Quaternary Research 18, 152–173.

Bull, W.B., 1991. Geomorphic Response to Climate Change. Oxford University Press, Oxford. p. 329.

Chatters, J.C., Hoover, K.A., 1992. Response of the Columbia River fluvial system to Holocene climate change. Quaternary Research 37, 42–59.

Chen, K., Bowler, J.M., 1986. Late Pleistocene evolution of salt lakes in the Qaidam Basin, Qinghai Province, China. Palaeogeography, Palaeoclimatology, Palaeoecology 54, 87–104.

Chen, Y.C., Sung, Q.C., Cheng, K.Y., 2003. Along-strike variations of morphotectonic features in the Western Foothills of Taiwan: tectonic implications based on stream-gradient and hypsometric analysis. Geomorphology 56, 109–137.

Colin, K.B., 2002. Paraglacial geomorphology. Quaternary Science Reviews 21, 1935–2017.

Cui, Z.J., Wu, Y.Q., Ge, D.K., Liu, G.N., 1999. Environmental change of Kunlun pass area since Quaternary. Marine Geology and Quaternary Geology 19, 53–62 (in Chinese with English abstract).

Cui, Z.J., Wu, Y.Q., Liu, G.N., Ge, D.K., Pang, Q.Q., Xu, Q.H., 1998. On Kunlun-Yellow River tectonic movement. Science in China 41, 592–600.

Finkel, R.C., Owen, L.A., Barnard, P.L., Caffee, M.W., 2003. Beryllium-10 dating of Mount Everest moraines indicates a strong monsoonal influence and glacial synchroneity throughout the Himalaya. Geology 31, 561–564.

Fisk, H.N., 1951. Loess and Quaternary geology of the Lower Mississippi Valley. Journal of Geology 59, 333–356.

Frechen, M., Schweitzer, U., Zander, A., 1996. Improvements in sample preparation for the fine grain technique. Ancient Thermoluminescence 14, 15–17.

Gao, H.S., Pan, B.T., Wu, G.J., Li, J.J., Li, B.Y., Burbank, D., Ye, Y.G., 2005. Age and genesis of alluvial terraces in east Qilian Mountains. Scientia Geographica Sinica 25, 197–202 (in Chinese with English abstract).

Godfrey-Smith, D.I., Huntley, D.J., Chen, W.H., 1988. Optical dating studies of quartz and feldspar sediment extracts. Quaternary Science Reviews 7, 373–380.

Hack, J.T., 1973. Drainage adjustment in the Appalachians. In: Morisawa, M. (Ed.), Fluvial Geomorphology. State University of New York, Binghamton, pp. 51–69.

Hans-Joachim, P., Bernd, W., Zhang, H.C., 1995. Lake evolution in the Tengger desert, northwestern China, during the last 40, 000 years. Quaternary Research 44, 171–180.

Hsieh, M.L., Knuepfer, P.L.K., 2001. Middle-late Holocene river terraces in the Erhjen River Basin, southwestern Taiwan – implications of river response to climate change and active tectonic uplift. Geomorphology 38, 337–372.

Hu, D.S., Zhang, H.J., Li, B.Y., Weng, J.C., 2002. Paleoclimatic oscillation events of the Dryas period: evidence from the record of lake records of lake sediments in the interior of the Qinghai-Tibet Plateau. Acta Geologica Sinica 76, 272–278 (in Chinese with English abstract).

Jia, Y.L., Shi, Y.F., Wang, S.M., Jiang, X.Z., Li, S.J., Wang, A.J., Li, X.S., 2001. Lake-expanding events in the Tibetan Plateau since 40 ka BP. Science in China 44 (Suppl.), 301–315.

Kong, P., Na, C.G., Flink, D., Huang, F.X., 2006. Cosmogenic ^{10}Be Dating of Moraine in Tianshan, Central Asia. INQUA Workshop on Timing and Nature of Mountain Glaciation. Xining, China, p. 30 (abstract).

Li, C.A., Luo, M.S., Yu, Q.W., Wang, Y.B., 1997. A preliminary study on sediment, geomorphology and environmental evolution of late Cenozoic in eastern Kunlun. Earth Science – Journal of China University of Geosciences 22, 347–351 (in Chinese with English abstract).

Li, H.B., Van der Woerd, J., Tapponnier, P., Klinger, Y., Qi, X.X., Yang, J.S., Zhu, Y.T., 2005. Slip rate on the Kunlun fault at Hongshui Gou, and recurrence time of great events comparable to the 14/11/2001, Mw$\sim$7.9 Kokoxili earthquake. Earth and Planetary Science Letters 237, 285–299.

Li, J.J., Fang, X.M., Ma, H.Z., Zhu, J.J., Pan, B.T., Chen, H.L., 1996. Geomorphologic evolution of upper reach of the Yellow River and Late Cenozoic uplift of Qinghai-Xizang plateau. Science in China 26, 316–322.

Li, Y.F., Zhang, Q.S., Li, B.Y., Gasse, F., 1994. Ostracod fauna and environmental changes during the past 17,000 years in the western Tibet. Acta Geographica Sinica 49, 46–54 (in Chinese with English abstract).

Lu, Y.C., Wang, X.L., Wintle, A.G., 2007. A new OSL chronology for dust accumulation in the last 130, 000 yr for the Chinese Loess Plateau. Quaternary Research 67, 152–160.

Lu, Y.C., Zhang, J.Z., Xie, J., 1988. Thermoluminescence dating of loess and palaeosoils from the Lantian section, Shanxi province, China. Quaternary Science Reviews 7, 245–250.

Mackin, J.H., 1948. Concept of the graded stream. Geological Society of America Bulletin 59, 463–512.

Maddy, D., Bridgland, D.R., Westaway, R., 2001. Uplift-driven valley incision and climate-controlled terrace development in the Thames Valley, UK. Quaternary International 79, 23–36.

Merritts, D.J., Vincent, K.R., Wohl, E.E., 1994. Long river profiles, tectonism and eustasy: a guide to interpreting fluvial terraces. Journal of Geophysical Research 99, 14031–14050.

Owen, L.A., Finkel, R.C., Caffee, M.W., Gualtieri, L., 2002. Timing of multiple glaciations during the late Quaternary in the Hunza Valley, Karakoram Mountains, Northern Pakistan: defined by cosmogenic radionuclide dating of moraines. Geological Society of America Bulletin 114, 593–604.

Owen, L.A., Finkel, R.C., Ma, H.Z., Barnard, P.L., 2006. Late Quaternary landscape evolution in the Kunlun Mountains and Qaidam Basin, Northern Tibet: A framework for examining the links between glaciation, lake level changes and alluvial fan formation. Quaternary International 154–155, 73–86.

Pachur, H.J., Wunnemann, B., Zhang, H., 1995. Lake evolution in the Tengger Desert, northwestern China, during the last 40, 000 years. Quaternary Research 44, 171–180.

Prescott, J.R., Hutton, J.T., 1994. Cosmic ray contributions to dose rates for luminescence and ESR dating: Large depths and long-term time variations. Radiation Measurements 23, 497–500.

Rees-Jones, J., 1995. Optical dating of young sediments using fine-grain quartz. Ancient TL 13, 9–14.

Rendell, H.M., Webster, S.E., Sheffer, N.L., 1994. Underwater bleaching of signals from sediment grains: new experimental data. Quaternary Geochronology 13, 433–435.

Seddon, M.B., Holyoak, D.T., 1985. Evidence of sustained regional permafrost during deposition of fossiliferous Late Pleistocene river sediments at Stanton Harcourt (Oxfordshire, England). Proceedings of the Geological Association 96, 53–71.

Shen, J., Liu, X.Q., Matsumoto, R., Wang, S.M., Yang, X.D., 2005. A high-resolution climatic change since the Late Glacial Age inferred from multi-proxy of sediments in Qinghai Lake. Science in China 48, 742–751.

Shi, Q., Chen, F.H., Zhu, Y., Madsen, D., 2002. Lake evolution of the terminal area of Shiyang River drainage in arid China since the last glaciation. Quaternary International 93–94, 31–43.

Shi, Y.F., Yao, T.D., 2006. MIS 3b (54$\sim$44 ka BP) Cold Period and Glacial Advance in Middle and Low Latitudes. INQUA Workshop on Timing and Nature of Mountain Glaciation. Xining, China, p. 34 (abstract).

Shi, Y.F., Yu, G., Liu, X.D., Li, B.Y., Yao, T.D., 2001. Reconstruction of the 30–40 ka BP enhanced Indian monsoon climate based on geologic records from the Tibetan Plateau. Palaeogeography, Palaeoclimatology, Palaeoecology 169, 69–83.

Starkel, L., 2003. Climatically controlled terraces in uplifting mountain areas. Quaternary Science Reviews 22, 2189–2198.

Thompson, L.G., Yao, T.D., Davis, M.E., Henderson, K.A., Mosley-Thompson, E., Lin, P.N., Beer, J., Synal, H.A., Cole-Dai, J., Bolzan, J.F., 1997. Tropical climate instability: the last glacial cycle from a Qinghai-Tibetan ice core. Sciences 276, 1821–1825.

Van der Woerd, J., Ryerson, F.J., Tapponnier, P., Gaudemer, Y., Finkel, R., Meriaux, A.S., Caffee, M., Zhao, G.G., He, Q.L., 1998. Holocene left-slip rate determined by cosmogenic surface dating on the Xidatan segment of the Kunlun fault (Qinghai, China). Geology 26, 695–698.

Vandenberghe, J., 1995. Timescales, climate and river development. Quaternary Science Reviews 14, 631–638.

Vandenberghe, J., 2003. Climate forcing of fluvial system development: an evolution of ideas. Quaternary Science Reviews 22, 2053–2060.

Wang, A., Wang, G.C., Xiang, S.Y., 2003. Characteristics of river terraces in north slope of eastern Kunlun Mountains and their relationship with plateau uplift. Earth Science – Journal of China University of Geosciences 28, 675–679 (in Chinese with English abstract).

Wang, A., Wang, G.C., Xie, D.F., Liu, D.M., 2006. Fission track geochronology of the Xiaonanchuan pluton and the morphotectonic evolution of eastern Kunlun since late Miocene. Journal of China University of Geosciences 17, 302–309 (English edition).

Wang, G.C., Yang, W.R., Ma, H.D., Wang, A., 2005a. Comparing of the tectonic uplift since Late Cenozoic between the East and West Kunlun Mountains. Earth Science Frontiers 12, 157–166 (in Chinese with English abstract).

Wang, N.L., Yao, T.D., Thompson, L.G., Henderson, K.A., 2002. Record of cold event in Early Holocene of Guliya ice core. Chinese Science Bulletin 47, 818–823 (in Chinese).

Wang, P., Lu, Y.C., Chen, J., 2004a. Optical stimulated luminescence (OSL) dating of Late Pleistocene terrace deposits in the eastern segment of the Altyn Tagh fault and its tectonic implication. Seismology and Geology 26, 716–726 (in Chinese with English abstract).

Wang, Q.L., Wang, J.H., Zhu, G.Z., Cui, D.X., Wang, W.P., Chen, Z.S., Song, Z.S., 2004b. Vertical deformations of the eastern Kunlun fault zone and west of Kunlun Mountain pass Ms8.1 earthquake. Seismology and Geology 26, 273–280 (in Chinese with English abstract).

Wang, S.L., Bian, C.Y., 1993. The involutions and their palaeoclimatic significance in the Nachi Tai region along the Qinghai-Xizang highway. Geographical Research 12, 94–100 (in Chinese with English abstract).

Wang, X.L., Lu, Y.C., Li, X.N., 2005b. Luminescence dating of fine-grained quartz in Chinese loess-simplified multiple aliquot regenerative-dose (MAR) protocol. Seismology and Geology 27, 615–623 (in Chinese with English abstract).

Wang, Y., Wang, J., Chi, Z.Q., Xiao, X.C., Zhang, Z.C., 2004c. Formation of Keriya River terraces and uplift of Western Kunlun. Ningxia Engineering Technology 3, 207–209 (in Chinese with English abstract).

Wu, Q.L., Yang, T.B., 2006. A first terrace formation in upper reaches of Wanchuan River in Lanzhou, and its explanation. Quaternary Sciences 26, 495 (in Chinese with English abstract).

Wu, Y.Q., Cui, Z.J., Liu, G.N., Ge, D.K., Yin, J.R., Xu, Q.H., Pang, Q.Q., 2001. Quaternary geomorphological evolution of the Kunlun Pass area and uplift of the Qinghai-Xizang (Tibet) Plateau. Geomorphology 36, 203–216.

Yao, T.D., Thompson, L.G., Shi, Y.F., Qin, D.H., Jiao, K.Q., Yang, Z.H., Tian, L.D., Mosley-Thompson, E., 1997. Climate variation since the Last Interglaciation recorded in the Guliya ice core. Science in China 40, 662–668.

Yi, C.L., Owen, L.A., Yang, J.Q., Li, D.W., Jiao, K.Q., Zhen, B.X., Li, S.J., Liu, K.X., Ding, X.F., Fu, D.P., 2006. An Assessment of the Radiocarbon Dating of Glacial Landforms in Tibet and the Bordering Mountains. INQUA Workshop on Timing and Nature of Mountain Glaciation. Xining, China, p. 41 (abstract).

Yin, G.M., Zhao, H., Lu, Y.C., Chen, J., Shen, J., 1999. The comparison of luminescent paleodoses of different sediments. Seismology and Geology 21, 170–186 (in Chinese with English abstract).

Zhang, H., Wuennemann, B., Ma, Y., Peng, J., Pachur, H.J., Li, J., Qi, Y., Chen, G., Fang, H., Feng, Z., 2002. Lake level and climate changes between 42, 000 and 18, 000 ^{14}C yr B.P. in the Tengger Desert, northwestern China. Quaternary Research 58, 62–72.

Zhao, Z.M., Li, R.S., 2006. Evolutionary characteristics of river and lake terraces in different areas of the Northern Qinghai-Tibet Plateau. Geological Bulletin of China 25, 221–225 (in Chinese with English abstract).

Zheng, D., 1999. Physical geography in Karakoram-Kunlun Mountains pp. 32–37. Science Press, Beijing (in Chinese).

Zheng, M.P., Meng, Y.F., Wei, L.J., 2000. Evidence of the pan-lake stage in the period of 40–28 ka BP on the Qinghai-Tibet Plateau. Acta Geologica Sinica 74, 266–272 (English edition).

Zheng, M.P., Yuan, H.R., Zhao, X.T., Liu, X.F., 2006. The Quaternary pan-lake (overflow) period and paleoclimate on the Qinghai-Tibet Plateau. Acta Geologica Sinica 80, 169–180 (in Chinese with English abstract).

Zheng, R.Z., Wei, X.X., Wang, F., Li, J.P., Ji, F.J., 2004. Terraces and tectonic uplifts at Yandantu and Changcaogou of the Altun northern marginal fault. Seismology and Geology 126, 189–199 (in Chinese with English abstract).